

HOSTED BY

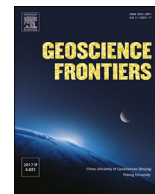


ELSEVIER

Contents lists available at ScienceDirect

China University of Geosciences (Beijing)

Geoscience Frontiers

journal homepage: www.elsevier.com/locate/gsf

Research Paper

Validation of basaltic glass adsorption capabilities from geothermal arsenic in a basaltic aquifer: A case study from Bjarnarflag power Station, Iceland

K.C. Weaver^{a,b,*}, M.A. Hoque^{a,c}, S.M. Amin^d, S.H. Markússon^e, A.P. Butler^a^a Department of Civil and Environmental Engineering, Imperial College London, London, SW7 2BU, United Kingdom^b School of Geography, Environment and Earth Sciences, Victoria University of Wellington, Wellington, New Zealand^c School of Earth and Environmental Sciences, University of Portsmouth, Portsmouth PO1 3QL, United Kingdom^d Gas Sustainability Technology, Group Research and Technology, Project Delivery and Technology, Petronas, Malaysia^e Landsvirkjun, Háaleitisbraut 68, 103 Reykjavík, Iceland

ARTICLE INFO

Article history:

Received 6 July 2017

Received in revised form

6 October 2018

Accepted 14 January 2019

Available online xxx

Keywords:

Geothermal

Groundwater

Hydrogeochemistry

Arsenic

Modelling

ABSTRACT

Arsenic is a carcinogen known for its acute toxicity to organisms. Geothermal waters are commonly high in arsenic, as shown at the Bjarnarflag Power Plant, Iceland ($\sim 224 \mu\text{g/kg}$ of solvent). Development of geothermal energy requires adequate disposal of arsenic-rich waters into groundwater/geothermal systems. The outcome of arsenic transport models that assess the effect of geothermal effluent on the environment and ecosystems may be influenced by the sensitivity of hydraulic parameters. However, previous such studies in Iceland do not consider the sensitivity of hydraulic parameters and thereby the interpretations remain unreliable. Here we used the Lake Mývatn basaltic aquifer system as a case study to identify the sensitive hydraulic parameters and assess their role in arsenic transport. We develop a one-dimensional reactive transport model (PHREEQC ver. 2.), using geochemical data from Bjarnarflag, Iceland.

In our model, arsenite (H_3AsO_3) was predicted to be the dominant species of inorganic arsenic in both groundwater and geothermal water. Dilution reduced arsenic concentration below $\sim 5 \mu\text{g/kg}$. Adsorption reduced the residual contamination below $\sim 0.4 \mu\text{g/kg}$ at 250 m along transect. Based on our modelling, we found volumetric input to be the most sensitive parameter in the model. In addition, the adsorption strength of basaltic glass was such that the physical hydrogeological parameters, namely: groundwater velocity and longitudinal dispersivity had little influence on the concentration profile.

© 2019, China University of Geosciences (Beijing) and Peking University. Production and hosting by Elsevier B.V. This is an open access article under the CC BY-NC-ND license (<http://creativecommons.org/licenses/by-nc-nd/4.0/>).

1. Introduction

Geothermal heat is mined from the ground, often producing waste-water. These waste-waters are enriched in silica, dissolved hydrogen sulphide, carbon dioxide, trace metals such as lead, copper, zinc and mercury, and trace metalloids such as arsenic (Fridleifsson, 2001). Geothermal water can be re-injected into subsurface reservoirs or discharged into surface drainage systems, using dilution to reduce the impact of harmful components

(Robinson et al., 1995). However, the disposal of geothermal water can increase arsenic concentration leading to exceedance of guideline values of drinking ($>0.01 \text{ mg/kg}$ of solvent) (World Health Organisation, 2011) and environmental water quality ($>0.1 \text{ mg/kg}$ of solvent) (Webster and Nordstrom, 2003).

Arsenic has several oxidation states, with the most common forms in groundwater being the inorganic oxyanions of As^{3+} (trivalent arsenite) and As^{5+} (pentavalent arsenate). Redox potential coupled with pH is the most important factors controlling arsenic speciation. According to equilibrium thermodynamic calculations, As^{3+} is prevalent in strongly reducing conditions, whereas As^{5+} is dominant in oxidising conditions (Smedley and Kinniburgh, 2002). Arsenic is one of the most carcinogenic and toxic substances in surface and groundwaters (Ravenscroft et al., 2009). As^{5+} inhibits oxidative phosphorylation in the ATP energy

* Corresponding author. School of Geography, Environment and Earth Sciences, Victoria University of Wellington, Cotton Building, Kelburn Parade, Wellington, 6012, New Zealand.

E-mail address: konradweaver@hotmail.co.uk (K.C. Weaver).

Peer-review under responsibility of China University of Geosciences (Beijing).

<https://doi.org/10.1016/j.gsf.2019.01.001>

1674-9871/© 2019, China University of Geosciences (Beijing) and Peking University. Production and hosting by Elsevier B.V. This is an open access article under the CC BY-NC-ND license (<http://creativecommons.org/licenses/by-nc-nd/4.0/>).

cycle while As^{3+} replaces sulphur in thiol groups which inhibits protein function (Squibb and Fowler, 1983).

Globally the principal cause of high arsenic concentration in the subsurface is the reductive dissolution of hydrous iron oxides (Nickson et al., 1998; Welch et al., 2000; Ravenscroft et al., 2009; Fendorf et al., 2010), oxidation of arsenic-bearing sulphides and desorption of arsenic due to an increased pH in oxidising aquifer conditions (Ravenscroft et al., 2009), and hydrothermal fluids with higher dielectrical constant S enabling leaching of arsenic from host rock (Webster and Nordstrom, 2003). According to studies by Arnórsson (2003), arsenic is highly mobile within shallow basaltic groundwaters with temperatures up to 90 °C. Arsenic concentration increases in groundwaters with higher temperatures and longer residence times which reflect on an increasing water/rock ratio. Indeed, the mixing of geothermal water with groundwater in basaltic settings, increases arsenic concentrations (Robinson et al., 1995).

The primary cause for the retardation of arsenate and arsenite transport in the subsurface is adsorption on iron oxides and hydroxides, even at low concentrations (Welch et al., 2000; Smedley and Kinniburgh, 2002; Sracek et al., 2004). Arsenate and arsenite have optimal adsorption affinities at pH 4 and 7 respectively (Pierce and Moore, 1982; Webster and Nordstrom, 2003; Sracek et al., 2004). High pH environments (>8.5) can cause desorption and dissolution of these compounds and increase mobility (Dzombak and Morel, 1990; Smedley and Kinniburgh, 2002; Sracek et al., 2004; Willis et al., 2011). In oxidizing conditions, hydrous iron oxides are stable and arsenic adsorption occurs (Ferguson and Gavis, 1972). Clay, organic matter, hydrous aluminium and manganese oxides are also adsorbents (Smedley and Kinniburgh, 2002; Webster and Nordstrom, 2003; Sracek et al., 2004).

Globally, geothermal waters are known to be high in arsenic. Icelandic environmental regulations set environmental limits for the concentration of arsenic-rich waters (Umhverfisstofnun, 1999). Arsenic-transport modelling has been accomplished on the Nesjavellir geothermal power plant in southern Iceland. However, sensitivity analysis of hydraulic parameters in the model were not conducted (Sigfusson et al., 2011), leaving the conclusion unreliable. Furthermore, no arsenic-transport modelling has been completed in the area to the East of Lake Mývatn.

We developed a one-dimensional reactive transport model using PHREEQC ver. 2 (Parkhurst and Appelo, 1999), incorporating field hydro-geochemistry data coupled with previously published (Sigfusson et al., 2008) laboratory-based adsorption coefficients. We conducted sensitivity analyses on arsenic transport modelling with the following parameters; volumetric input, basalt-glass interaction, groundwater velocity and dispersivity. The purpose of this study was to evaluate reinjection as a viable solution for geothermal water disposal. This culminated in the production of three scenarios for predictability of future arsenic concentrations. The results obtained in this study may eventually be utilised for other arsenic-rich geothermal production water localities world-wide.

2. Tectonics, geothermal and hydrogeological setting

2.1. Tectonic setting

Iceland is situated on the plate boundary between the North American and Eurasian plate. The plate boundary is marked by a rift zone which consists of several horsts and grabens and extends across Iceland (Thorarinsson, 1979; Gudmundsson et al., 2010). The Bjarnarflag Power Plant and the associated Námafjall geothermal field are located in this rift zone in North-East Iceland (Fig. 1).

The bedrock in the area surrounding Bjarnarflag consists of hyaloclastites, basaltic lavas, and glacial moraines (Fig. 1; Ólafsson, 1979a; Thorarinsson, 1979; De Zeeuw and Gislason, 1988). Hyaloclastite tuffs

were produced by the region's sub-glacial volcanic activity (Thóroddsson and Sigbjarnarson, 1983; De Zeeuw and Gislason, 1988). Glacier advancement associated with the Younger Dryas period (~11 ka), dominated the Mývatn-landscape in the last glacial period which produced extensive deposits of terminal moraines, sandur plains and other glacio-fluvial deposits (Gudmundsson et al., 1971; Thorarinsson, 1979). Following the Younger Dryas period, there were several episodes of volcanic activity. The outpouring of the Older and Younger Laxárhraun created Lake Mývatn and associated pseudo-craters (Thorarinsson, 1979; Ólafsson, 1979a). The Mývatn (1724–1729) and Krafla fires (1976–1980) produced extensive amounts of lava with fissure-type eruptions (Thorarinsson, 1979; Ólafsson, 1979a).

2.2. Geothermal exploitation

The Bjarnarflag Power Plant generates 18 GWh (gigawatt-hours) per year at present (Gudmundsson et al., 2010). As a result, 200 million tonnes of effluent waste-water have been discharged into the surrounding lavas over the past 40 years. The Bjarnarflag lagoon stores the geothermal water, before it infiltrates into the bedrock.

2.3. Hydrogeological regime

Lake Mývatn is in close proximity to the Bjarnarflag Power Plant (Fig. 1). The lake is listed as an important habitat for birds in the RAMSAR convention on wetlands (Ármannsson, 2005). A complex relationship is observed between: fish populations; waterfowl; benthic diatoms; filamentous green algae; blooms of cyanobacteria; phytoplankton and chironomids (Einarsson et al., 2004).

The shallow (≤ 4.2 m) eutrophic lake (~36.7 km²) has two components, a northern basin (~8.5 km²) and a southern basin (~28.2 km²) (Einarsson et al., 2004). The northern basin is fed by warm (~30–40 °C) artesian springs at ~11 m³/s, while the southern basin is fed by cold (~5 °C) artesian springs at ~17 m³/s, both located on the eastern shore (Ólafsson, 1979a; Vatnaskil, 2008). The water column is well mixed in summer, and thermally stratified during winter (Ólafsson, 1979a). The colder southern springs originate from the Dyngjujökull, Hvannfell and Lúdent mountains (Einarsson, 1972; Ármannsson et al., 1998), while warmer northern springs have locally sourced recharge (Arnason, 1977). Groundwater velocities vary over the study area. Warm waters near the Námafjall geothermal area travel at 0.33–0.81 m/min. Further away, cold waters travel at 0.61–2 m/min (Hauksdóttir et al., 2000).

The postglacial lava and scoria in the area are the most transmissive formations with a measured transmissivity of 2.5 m²/s (De Zeeuw and Gislason, 1988; Arnórsson, 1995). The inter-bedded scoria can be assumed to act as a homogeneous aquifer, while the basaltic lavas are more heterogeneous with varying porosity and pore sizes (De Zeeuw and Gislason, 1988; Gudmundsson et al., 2010). The hyaloclastites are heterogeneous with high porosity (0.60) but have variable permeability, and act as aquitards (Franzson et al., 2010).

Several tracer tests have followed groundwater flow to Lake Mývatn (Thóroddsson and Sigbjarnarson, 1983; Kristmannsdóttir et al., 2001) with 100 million fold dilution and two clear different modes of flow system between Bjarnarflag lagoon and Grjótagjá (Fig. 1; Hauksdóttir et al., 2000; Kristmannsdóttir et al., 2001; Ármannsson, 2005). A detailed summary of this work is given by Hauksdóttir et al. (2000).

It has been postulated that there are two different modes of flow in the system (Arnason, 1977; De Zeeuw and Gislason, 1988). One occurs at a depth of 1–3 km, where slow flows are directed by hydrostatic pressure in horizontal basaltic layers. The second flow pathway is faster, shallow (<30 m), and is determined by the fracture intensity of the area (Arnason, 1977).

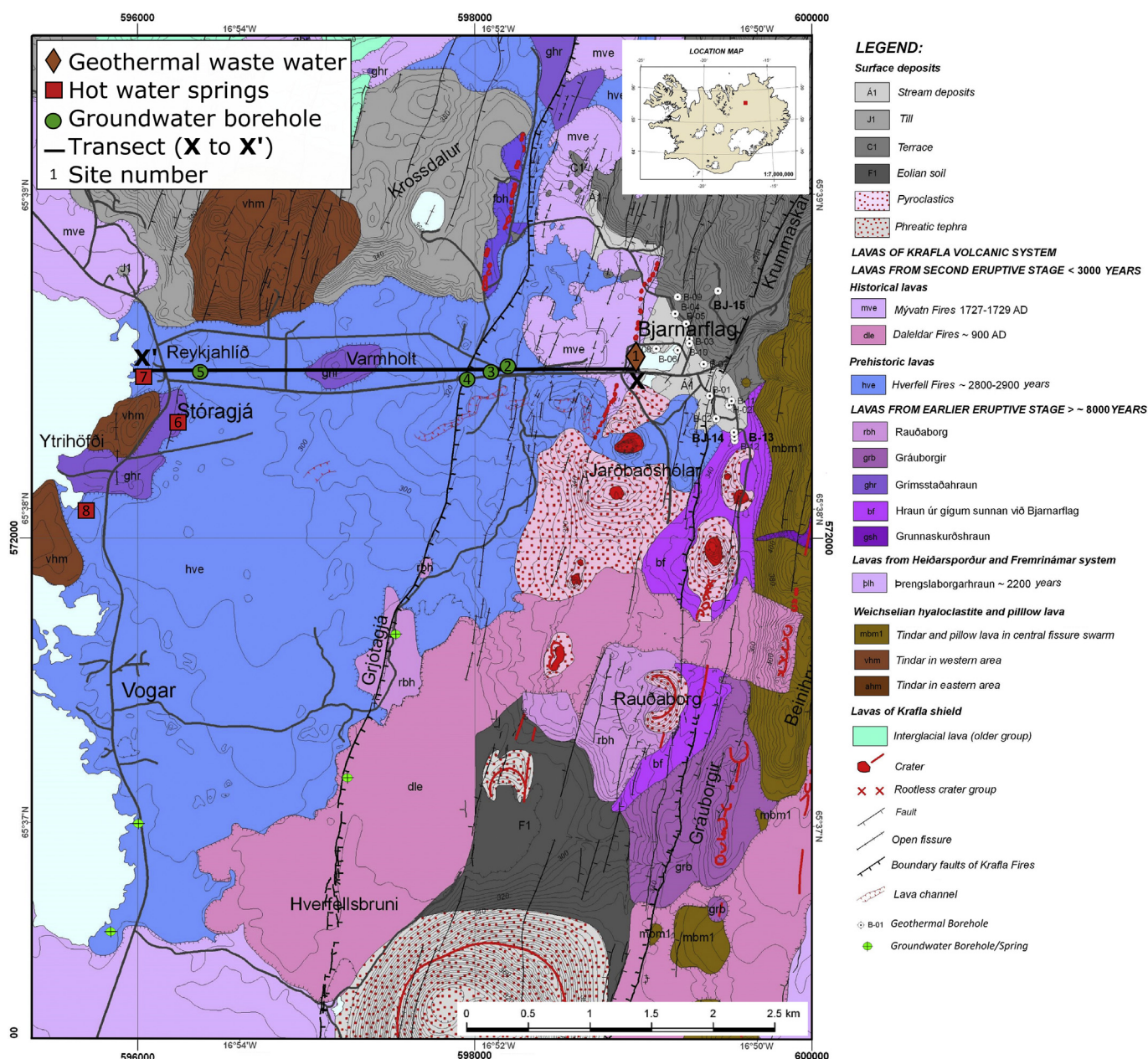


Figure 1. Geological map of the eastern shore of Lake Mývatn (Sæmundsson, 2010), along with the location of the sites where water samples have been taken. Inset map is the location of the study area in Iceland.

2.4. Water chemistry and fluid composition

The warmer springs have a pH of 8.3–8.6 (Ólafsson, 1979a), with a high concentration of dissolved solids due to hydrothermal leaching of the basalt and scoria rock formations. The warmer springs are saturated in calcium carbonate, and have a dissolved oxygen saturation of 80%–92% (Ólafsson, 1979b). The mixing of the Námafjall field geothermal effluent with the warm groundwater, has shifted the warm groundwater $\delta^{18}\text{O}$ (–11.58‰ to –11.92‰), which differs from the cold groundwater $\delta^{18}\text{O}$ (–12.72‰ to –13.03‰), sourced from the inland to the South of Lake Mývatn (Ármansson, 2005). The colder springs have a pH of 8.9–9.2, a low concentration of dissolved solids, a dissolved oxygen saturation of 69% to 82%, and are undersaturated in calcium carbonate (Ólafsson, 1979a).

2.5. Environmental regulation

Categories for surface effluent pollutants have been established for the protection of the biosphere in Iceland (Hauksson, 2013). The five categories for arsenic are: (i) very little or no risk to exposure, <0.4 µg/kg of solvent, (ii) small risk to exposure, 0.4–5 µg/kg of solvent, (iii) effect expected on sensitive ecosystem, 5–15 µg/kg of solvent, (iv) impact is expected, 15–75 µg/kg of solvent, (v) dilution needed in ecosystem, >75 µg/kg of solvent (Umhverfisstofnun, 1999).

3. Materials and methods

The Iceland Geological Survey (ISOR) has provided water-sampling chemistry data from 8 hydrological sites (Fig. 1 and

Table 1). The hydrological sites include: 3 hot water springs, 4 groundwater boreholes and 1 geothermal waste water sites. The sites have been sampled from 1978 to 2013, every 1 to 5 years. The arsenic concentration was relatively stable over this time period in all 3 hydrological site types. Therefore, for the relation of arsenic to chloride and temperature, all chemical analyses which measure these fluid properties were included. For the speciation and dilution modelling of the geothermal effluent in the groundwater, the groundwater composition was obtained primarily from Site 3 as

this groundwater site is in close proximity to the lagoon and the water-sampling data is the most recent (Fig. 1). Although Site 3 has the most recent water-sampling measurements, not all chemical components were measured at this site. Therefore, to provide a complete chemical profile for the dilution scenario, the most recent measurements from the nearest sites (Site 4, 5 and 8) were adopted (Table 1). The geothermal effluent composition was obtained from Site 1. Transport modelling of the arsenic concentration occurred along the transect X–X' shown in Fig. 1.

Table 1
Properties of 1D transport model in PHREEQC ver. 2. * = Site 4, ** = Site 5, *** = Site 8.

| 1D transport properties in PHREEQC | | | |
|--|----------------------------------|----------------------------------|----------------------------------|
| Number of cells | 30 | | |
| Cell length (m) | 100 | | |
| Pore volumes | 2167 | | |
| Shifts | 65,000 | | |
| Groundwater velocity (m/min) | 0.58 | | |
| Total simulation time (years) | 21.2 | | |
| Dispersivity (m) | 5 | | |
| Diffusion coefficient (m ² /s) | 1.16E-09 | | |
| Liquid in each cell (L) | 1 | | |
| Dilution factor (Effluent volume, m ³ /s) | 1:424 (0.026) | | |
| Solution composition | Groundwater (Site 3) | Geothermal water (Site 1) | Mixture (PHREEQC) |
| pH | 7.93 | 6.25 | 7.9274 |
| Temperature (°C) | 42 | 30 | 41.972 |
| Redox couple | S ⁶⁺ /S ²⁻ | S ⁶⁺ /S ²⁻ | S ⁶⁺ /S ²⁻ |
| pe | −4.7045 | −2.5011 | −4.7013 |
| Units | mg/kg of solvent | mg/kg of solvent | mg/kg of solvent |
| Al | 0.027* | 2.67 | 0.033 |
| As | 0.0001** | 0.224 | 0.0006 |
| CO ₂ | 75.5 | 0.6 | 75.4 |
| Ca | 19.58 | 2.48 | 19.55 |
| Cl | 23.17 | 60.2 | 23.27 |
| Cu | 0.0012** | 0.00181 | 0.0012 |
| F | 0.392 | 0.9 | 0.393 |
| Fe | 0.0025** | 0.691 | 0.0041 |
| K | 8.93 | 24.2 | 8.97 |
| Li | 0.0112** | 0 | 0.0112 |
| Mg | 3.51 | 1.11 | 3.5 |
| Mn | 0.0002** | 0.0005 | 0.0002 |
| Na | 75.91 | 115.7 | 76.04 |
| PO ₄ | 0.137*** | 0.169 | 0.137 |
| H ₂ S | 0.1* | 0.1 | 0.1 |
| SO ₄ | 114* | 171.5 | 114.1 |
| SiO ₂ | 115 | 256 | 115 |
| Zn | 0.0012** | 0.00572 | 0.0012 |
| Saturation indices | | | |
| SiO ₂ | −0.15 | 0.3 | −0.1462 |
| Chalcedony | 0.64 | 1.12 | 0.639 |
| Al(OH) ₃ | −2.72 | 0.96 | −2.6254 |
| Gibbsite | −0.17 | 3.61 | −0.0816 |
| Fe(OH) ₃ | −6.1 | −6.67 | −5.8888 |
| Pyrite | 5.69 | 8.24 | 5.9041 |
| FeS | −1.38 | −1.2 | −1.1684 |
| Basaltic glass | | | |
| (Sigfusson et al., 2011) | | | |
| Mass in each cell (kg) | 2.31 | | |
| Specific surface area (m ² g ^{−1}) | 1.5 | | |
| Surface sites (sites nm ^{−2}) | 4 | | |
| Arsenic surface reactions | Log K (25°C) | | |
| (Sigfusson et al., 2008) | | | |
| Glass = Basaltic glass | | | |
| As ^(V) | | | |
| 2Glass-OH + H ₃ AsO ₄ = (Glass-O) ₂ AsOOH + 2H ₂ O | 4.3 | | |
| 2Glass-OH + H ₃ AsO ₄ = (Glass-O) ₂ AsO ₂ + H ⁺ + 2H ₂ O | 2.3 | | |
| Glass-OH + H ₃ AsO ₄ = Glass-OAsO ₃ [−] + 2H ⁺ + H ₂ O | −2.4 | | |
| As ^(III) | | | |
| 2Glass-OH + H ₃ AsO ₃ = (Glass-O) ₂ AsOH + 2H ₂ O | 4.7 | | |
| Glass-OH + H ₃ AsO ₃ = Glass-H ₄ AsO ₄ | −2.78 | | |

3.1. Geochemical simulation

The fluid-rock interactions of a homogenous scoria were simulated using PHREEQC ver. 2: speciation, dilution and reactive transport modelling (Parkhurst and Appelo, 1999). These experiments were based on an ion-association aqueous model. The Debye-Hückel equation was used to calculate the activity coefficients of the species (Fig. 3). PHREEQC was supplemented with a thermodynamic database (phreeqc.dat) that provided equilibrium constants.

The mass-balance model used the latest groundwater model estimates of flow to the northern basin of Lake Mývatn, 11 m³/s (Vatnaskil, 2008), and the current average infiltration rate of the waste-water, 0.026 m³/s (Hauksson, 2013) (Fig. 2). The estimate of effluent yields a dilution factor of 1:424. Mixing with deeper geothermal water was excluded as a result of the inability to quantify such flows.

The simulations were started from a chemically, hydrologically and geometrically simplified batch system at equilibrium. The Advection-Reaction-Dispersion (ARD) equation was applied (Parkhurst and Appelo, 1999):

$$\frac{\partial C}{\partial t} = -v \frac{\partial C}{\partial x} + D_L \frac{\partial^2 C}{\partial x^2} - \frac{\partial q}{\partial t} \quad (1)$$

where t is time (s), C is concentration in water (mol/kgw), v is groundwater velocity (m/s), x is distance (m), D_L is the hydrodynamic dispersion coefficient (m²/s) and q is the concentration in the solid phase (mol/kgw in the pores).

The base model transport properties are listed in Table 1. The base model was represented by a 3000 m strip discretized into 30 cells, each being 100 m in length (Fig. 2). Each cell contained 1 litre of diluted geothermal water with a total of 18 aqueous components (Table 1). The domain was composed of homogeneous scoria with an initial porosity of 0.5, as flow was assumed to concentrate in these horizons (De Zeeuw and Gislason, 1988; Gudmundsson et al., 2010). A fixed mass of basaltic glass was assigned to each cell based on this porosity. We assumed a 50% interaction rate between the fluid and basaltic glass. The equilibrium constants for the arsenic-basaltic glass surface reactions (Sigfusson et al., 2008) were input into PHREEQC (Table 1). The arsenite diffusion coefficient (1.16×10^{-9} m²/s) was used since the redox conditions favoured this reduced form of arsenic (Fig. 5). A dispersivity value of 5 m was chosen to imitate a fractured-layered basaltic system (Schulze-Makuch, 2005 and references therein). The groundwater velocity of 0.58 m/min was obtained from tracer studies (Hauksdóttir et al., 2000), and represents the median velocity measured by tracer arrival times near the transect end (X') at Lake Mývatn.

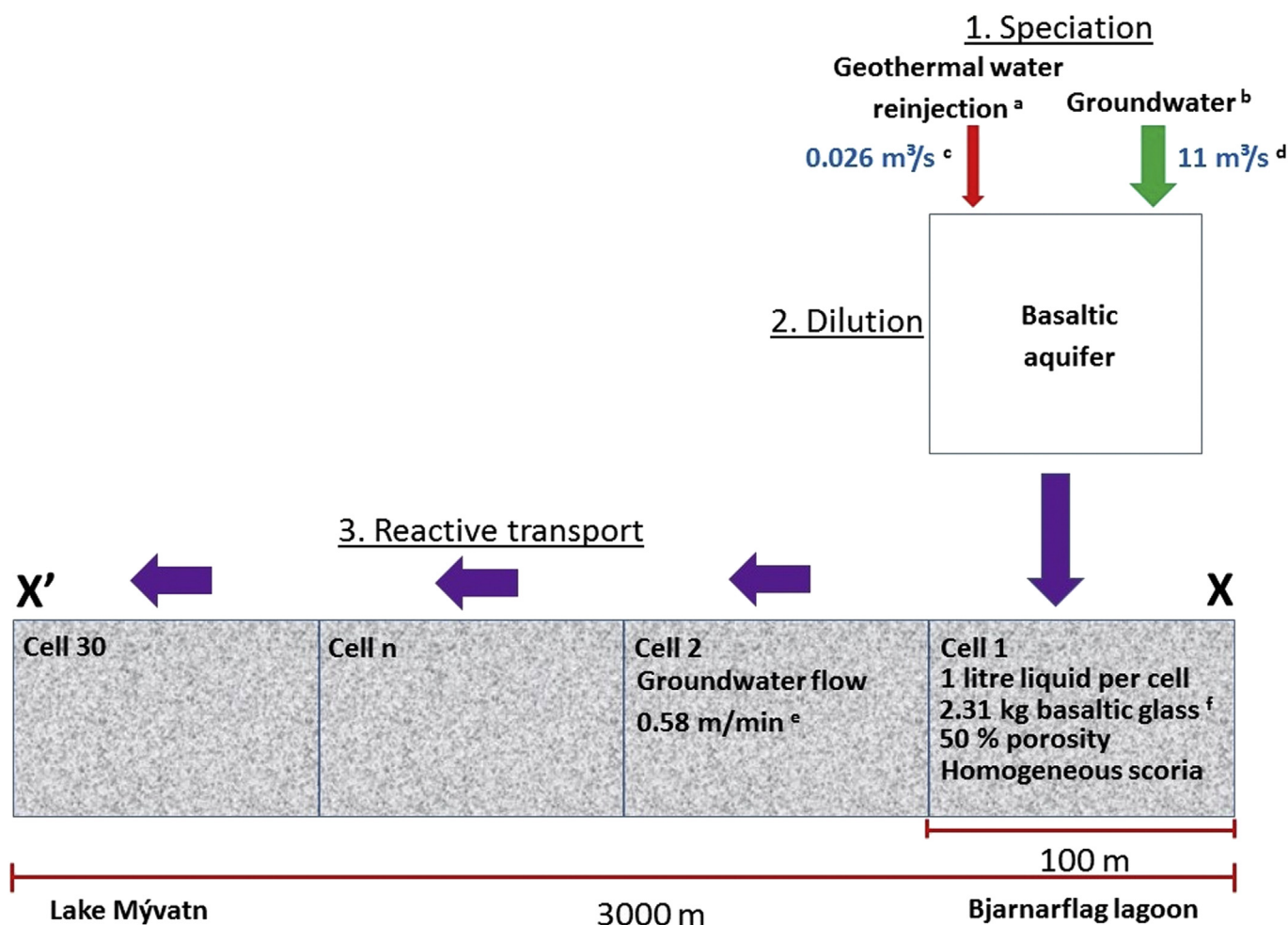


Figure 2. Diagrammatic representation of the methodology in PHREEQC: ^a Composition is provided (Hauksson, 2013); ^b Composition is provided by ISOR; ^c Geothermal waste production is provided as an arithmetic mean from 1977 to 2012 (Hauksson, 2013); ^d Groundwater flow rate provided from latest model (Vatnaskil, 2008); ^e Groundwater velocity based on tracer tests (Hauksdóttir et al., 2000). ^f Basaltic glass surface reactions provided (Sigfusson et al., 2008).

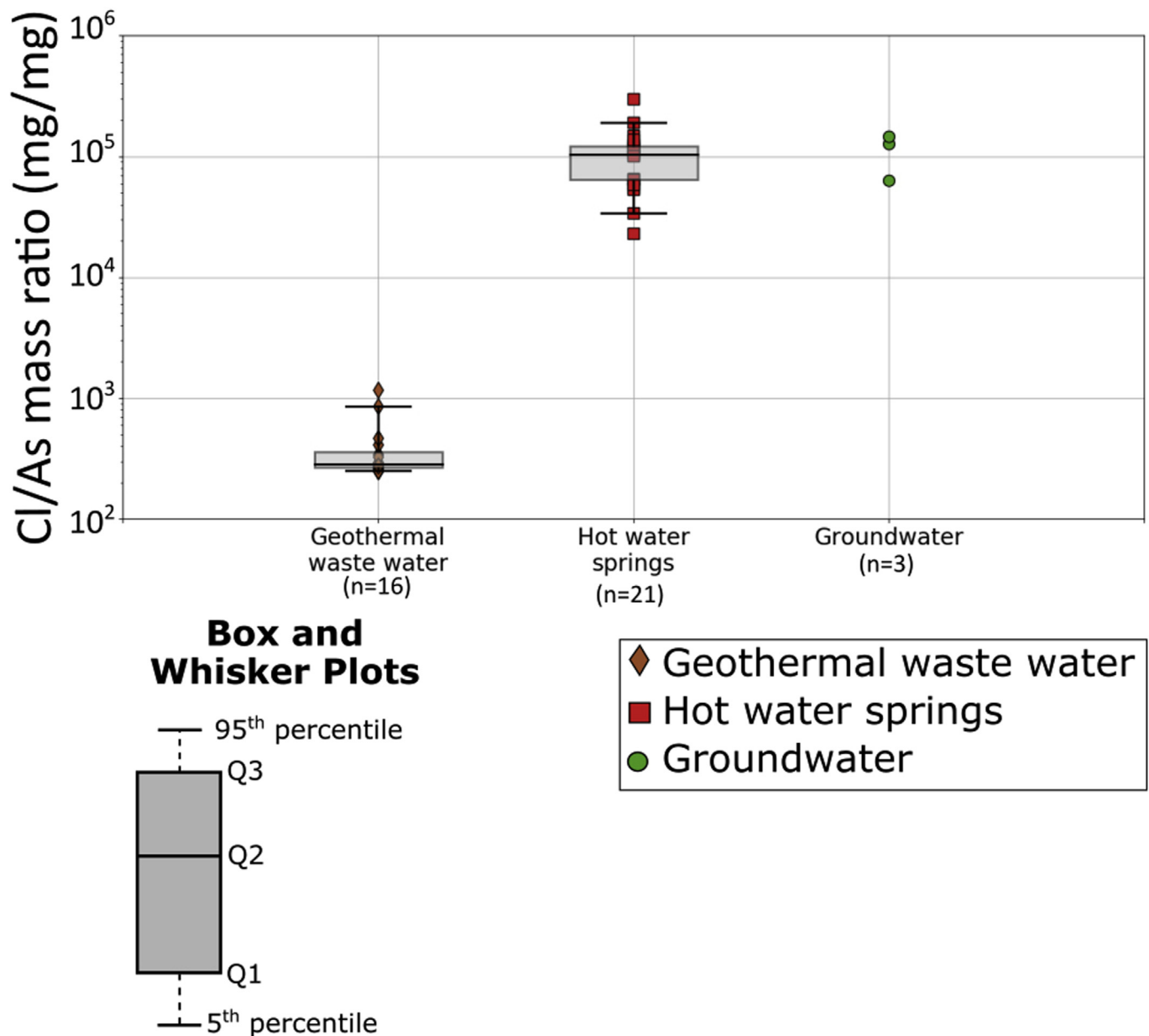


Figure 3. The chloride/arsenic ratio for the geothermal waste water, groundwater, and hot water springs sampled between 1978 and 2013. In an additional 36 instances, arsenic concentrations were below the detection limit (0.02 $\mu\text{g}/\text{kg}$ of solvent) in hot water springs. Not all chemical analyses over this period included measurements of chloride and arsenic. The locations of hydrological sites are shown in Fig. 1.

Four assumptions were made in the transport simulation:

- (1) Biological influences (Smedley and Kinniburgh, 2002) and competing ions were not considered in the model. This likely resulted in under-estimation of equilibration times (Sracek et al., 2004);
- (2) Geothermal and groundwater compositions remained constant and mixing was assumed instantaneous;
- (3) The arithmetic mean of the hot water springs and groundwater temperatures (Site 2–8) along the transect (X–X') (Fig. 1) is $\sim 30^\circ\text{C}$. Considering the simulated mixing of the geothermal effluent water and the groundwater (Table 1) did not change the groundwater temperature significantly, the basaltic glass interaction equilibrium constants derived at 25°C (Sigfusson et al., 2008) were used (Table 1);

- (4) Transport modelling was one dimensional in a homogeneous aquifer, thus avoiding heterogeneities in composition and structure.

Numerical dispersion has been known to occur in coarse grid models of PHREEQC. The robustness of the model was tested using alternative grid sizes (100 m, 250 m, 500 m) in a one-dimensional transport model (Fig. 6). Calibration of the model using arsenic was not possible due to a limited number of data points along the transect (X–X'). Only 3 arsenic measurements are available in close proximity to Lake Mývatn. No groundwater samples in the region pre-dated the first production of geothermal power at Bjarnarflag Power Plant. Therefore, geothermal water likely has already contributed to the base-line groundwater chemistry. A beneficial comparison of the model with independently obtained analytical

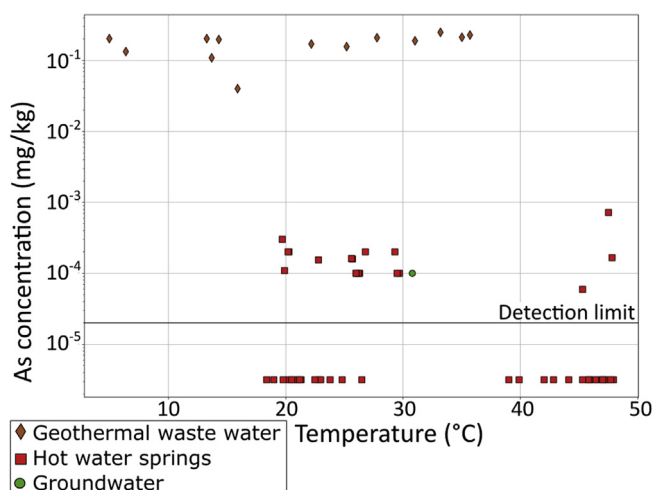


Figure 4. The relationship between arsenic and temperature in the geothermal waste water, groundwater, and hot water springs sampled between 1978 and 2013. Not all chemical analyses over this period included measurements of temperature and arsenic. The location of hydrological sites are shown in Fig. 1.

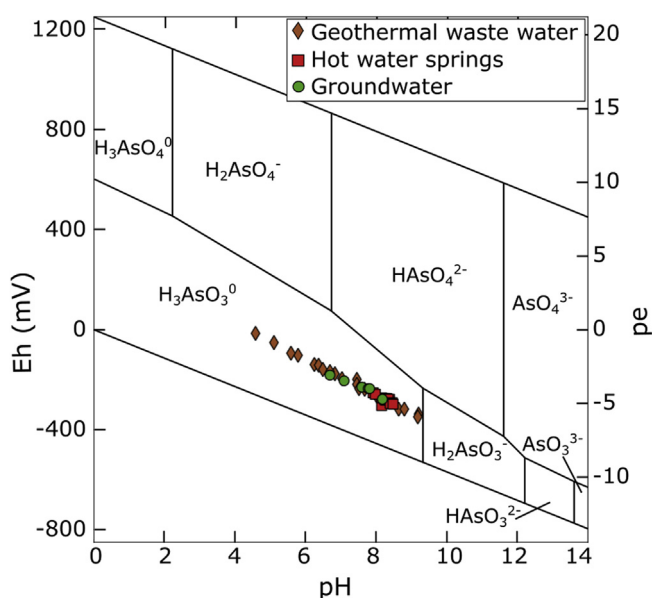


Figure 5. Arsenic speciation of geothermal waste water, hot water springs and groundwater, estimated by Eh and pH.

data was therefore not possible as data were not spatially or temporally comprehensive. This motivated an extensive sensitivity analysis of flow parameters.

This model builds upon the model on southern Iceland aquifer systems presented by Sigfusson et al. (2011), as we undertake an extensive sensitivity analysis to assess the significance of the flow parameters. In the sensitivity analysis four properties were varied: effluent volume, rock-water interaction, groundwater velocity, and dispersivity. The base model and each sensitivity analysis are simulated for 20 years, and the arsenic concentration is measured in each cell (cell 1 to 30). Considering the dynamic enthalpy of boreholes, effluent volume was reduced by half ($0.013 \text{ m}^3/\text{s}$), doubled ($0.052 \text{ m}^3/\text{s}$), and tripled ($0.078 \text{ m}^3/\text{s}$) to assess its sensitivity on the base model. These changes in effluent volume are far larger than natural fluctuations of effluent production between 1977 and 2012 (Hauksson, 2013). At 50% porosity (2.31 kg, Table 1), the interaction of the fluid with the basaltic glass, was reduced (achieved by

reducing the mass of basaltic glass in the transport model) until arsenic concentrations were increased (0.0003%, 7 mg). A range of groundwater velocities above and below 0.58 m/min (0.3, 0.75 and 1 m/min, Hauksdóttir et al., 2000) were simulated reflecting faster and slower flow pathways to Lake Mývatn. Variable dispersivity values (Schulze-Makuch, 2005) were assessed, which represent realistic heterogeneities in the field. A dispersivity value of 76 m (Souza and Voss, 1987) was chosen to reflect a layered basaltic system. Dispersivity values of 1, 0.1 and 0.01 m (Steele et al., 1989; Nimmer, 1998) were chosen to reflect a fractured basaltic system.

A set of three scenarios were considered which used parameter values conducive for likely contamination of Lake Mývatn. Scenario (1) included a dispersivity of 76 m relating to layered scoria flow. Scenario (2) further introduced a faster groundwater velocity of 1 m/min. Scenario (3) further included a three-fold increase in effluent volume re-injected (Table 2).

4. Results

4.1. Chemical and thermal relationships

Based on the chloride to arsenic (Cl/As) ratio (mg/mg), there are two distinct groups of subsurface water (Fig. 3). The geothermal waste waters have a Cl/As ratio of $<10^3$, and the groundwater, and hot water springs have a Cl/As ratio of $\sim 10^{4.1}$ to $\sim 10^{5.3}$.

Arsenic concentrations also highlight two distinct groups of subsurface water (Fig. 4). Arsenic concentrations in the geothermal waste waters are $\sim 10^{-1} \text{ mg/kg}$, and in the groundwater and hot water springs are $\sim 10^{-4} \text{ mg/kg}$. There are numerous instances where arsenic concentrations are below the detection limit ($0.02 \text{ } \mu\text{g/kg}$ of solvent) in the hot water springs. There is no clear correlation between temperature and arsenic concentration (Fig. 4).

4.2. Modelling output

4.2.1. Speciation

The pH and redox potential (Eh) can be used to estimate the major arsenic species present in a solution. Here, the Eh was estimated by the $\text{S}^{2-}/\text{S}^{6+}$ redox couple in PHREEQC (Fig. 5). The results show that the major arsenic species is H_3AsO_3^0 .

4.2.2. Dilution

The dilution simulation between the geothermal effluent and groundwater reduces the geothermal arsenic concentration significantly, to $\sim 0.6 \text{ } \mu\text{g/kg}$ of solvent, with zinc, copper and phosphate also being reduced (Table 1). Temperature and pH remain relatively constant in the groundwater system. The reduction potential decreases by 0.0032. Saturation indices of influential mineral phases largely remain in their groundwater saturation states (Table 1).

4.2.3. Reactive transport – Numerical dispersion

In the transport modelling, the coarser grid sizes computed higher concentrations along the transect (X–X'); yet, all three simulations retained similar temporal and spatial behaviour of arsenic concentration (Fig. 6). Moreover, the variations were not sufficiently significant to cross environmental categorical thresholds.

4.2.4. Reactive transport – Sensitivity

The sensitivity analysis assesses the significance of effluent reinjection volume, the basalt-glass-fluid interaction extent, groundwater velocities, and dispersivity. Increased effluent reinjection volume raises the arsenic concentration profile, and was considered the most sensitive parameter (Fig. 7a). A threefold increase in the geothermal effluent produced, increased the arsenic

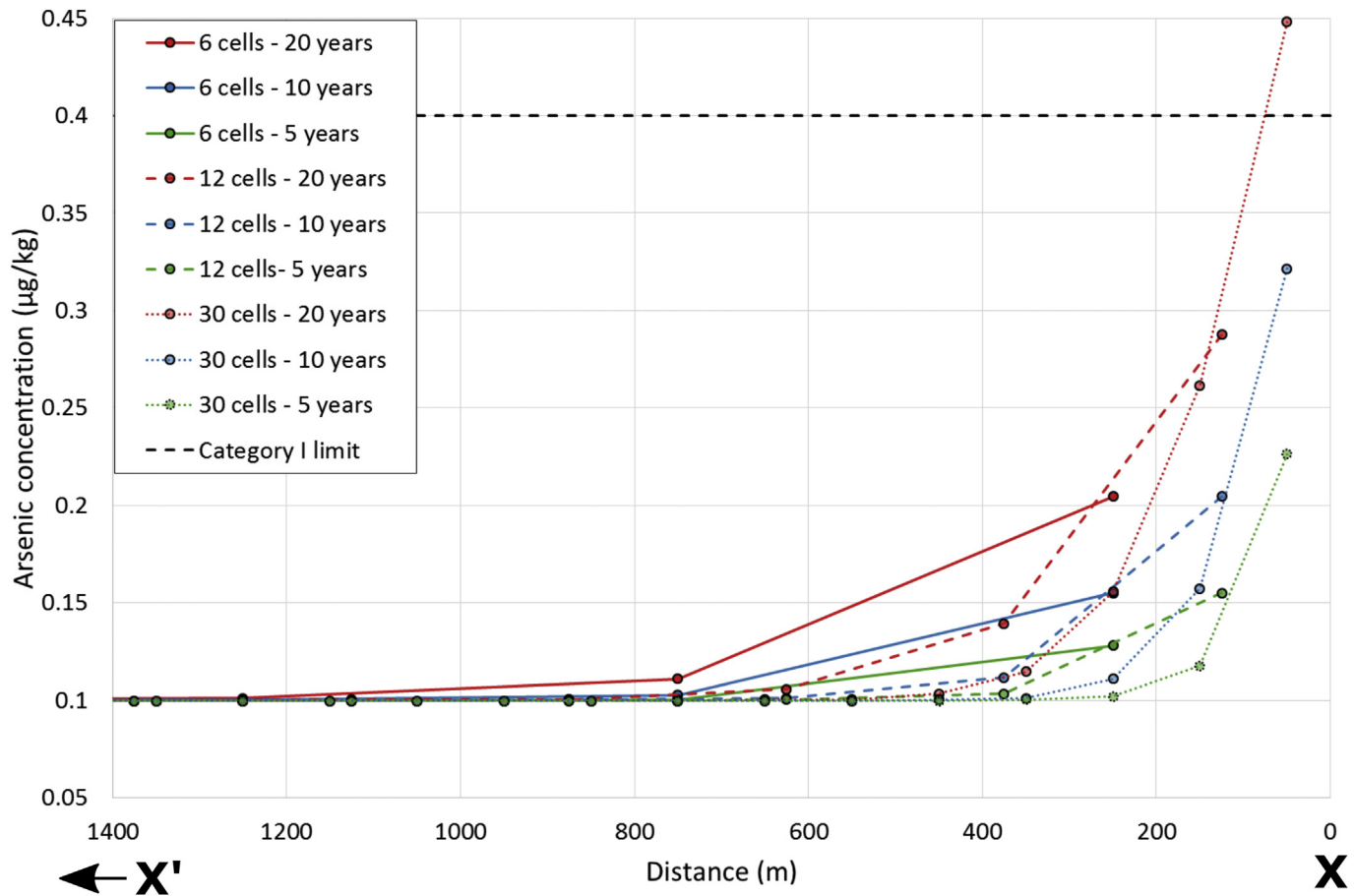


Figure 6. Comparison of grid resolution along transect (X–X'). A cell size of 100 m (30 cells), 250 m (12 cells), and 500 m (6 cells) were tested.

concentration at the start of the transport model by ~ 0.7 $\mu\text{g/kg}$ of solvent. Even with such unexpected high volumes of effluent, the arsenic concentration was still reduced below the Category I limit (0.4 $\mu\text{g/kg}$ of solvent) in the transport model, 300 m from the lagoon. The basalt-glass-fluid interaction extent, at a porosity of 0.5, was reduced from 50% until arsenic concentrations increased. Sensitivity is only observed at unrealistically low interaction levels (0.0003%) (Fig. 7b). A porosity of 0.0003% limits adsorption of arsenic, and sustains arsenic levels above base model concentrations until cell 10 to 12 (1–1.2 km from the lagoon). Along the transect, slower groundwater velocities had a greater impact on arsenic concentration decrease than increasing groundwater velocity did on arsenic concentration increase (Fig. 7c). An intensified fractured system, represented by reduced dispersivity (1 m, 0.1 m, 0.01 m), had no significant effect on the arsenic concentration profile. However, a larger dispersivity (76 m, Souza and Voss, 1987), replicating a layered scoria environment, caused an attenuation of arsenic concentration relative to other simulations, resulting in a lower concentration close to the lagoon and a higher concentration towards Lake Mývatn (Fig. 7d).

Table 2
Flow properties varied from the base model in scenarios 1, 2, and 3. Flow properties include dispersivity, groundwater velocity and effluent volume.

| 1D transport properties in PHREEQC | Base model | Scenario 1 | Scenario 2 | Scenario 3 |
|---|------------|------------|------------|------------|
| Dispersivity (m) | 5 | 76 | 76 | 76 |
| Groundwater velocity (m/min) | 0.58 | 0.58 | 1 | 1 |
| Effluent volume (m^3/s) | 0.026 | 0.026 | 0.026 | 0.078 |

4.2.5. Scenarios

Extensive sensitivity analysis has considered several variables in isolation. Subsequently, three scenarios were simulated over a 20 year period, with variations in the most significant parameters (Fig. 8). Scenario (2), which included the faster pore water velocity (1 m/min), predicted the highest concentration generally along the transect. The simulation for the base model and scenario (2), exceeded 0.4 $\mu\text{g/kg}$ of solvent in arsenic concentration. However, the concentration decreased below this limit at 100 m from the lagoon. The base model and scenarios (1) and (2) all reached a minimum concentration of 0.1 $\mu\text{g/kg}$ of solvent by ~ 350 m from the lagoon.

Scenario (3) simulated a three-fold increase in effluent volume and thus was expected to produce significantly higher concentrations of arsenic along the profile (Fig. 8b). Scenario (3) exceeded the Category (I) limit (0.4 $\mu\text{g/kg}$ of solvent) until ~ 260 m. As with the other scenarios, in Scenario (3) the arsenic reached the minimum concentration of 0.1 $\mu\text{g/kg}$ of solvent by ~ 700 m.

5. Discussion

5.1. Geochemistry

In the study area, arsenic concentrations are separated into two different groups (Figs. 3 and 4). Arsenic concentrations are significantly higher in the geothermal waste waters (10^{-1} mg/kg of solvent) than the groundwater, and hot water springs (10^{-4} mg/kg of solvent). This enrichment in arsenic reflects extensive water-rock interactions which occur at high temperatures (Arnórsson, 2003). However, there is no clear relationship

Arsenic concentration after 20 year simulation along transect (X to X')

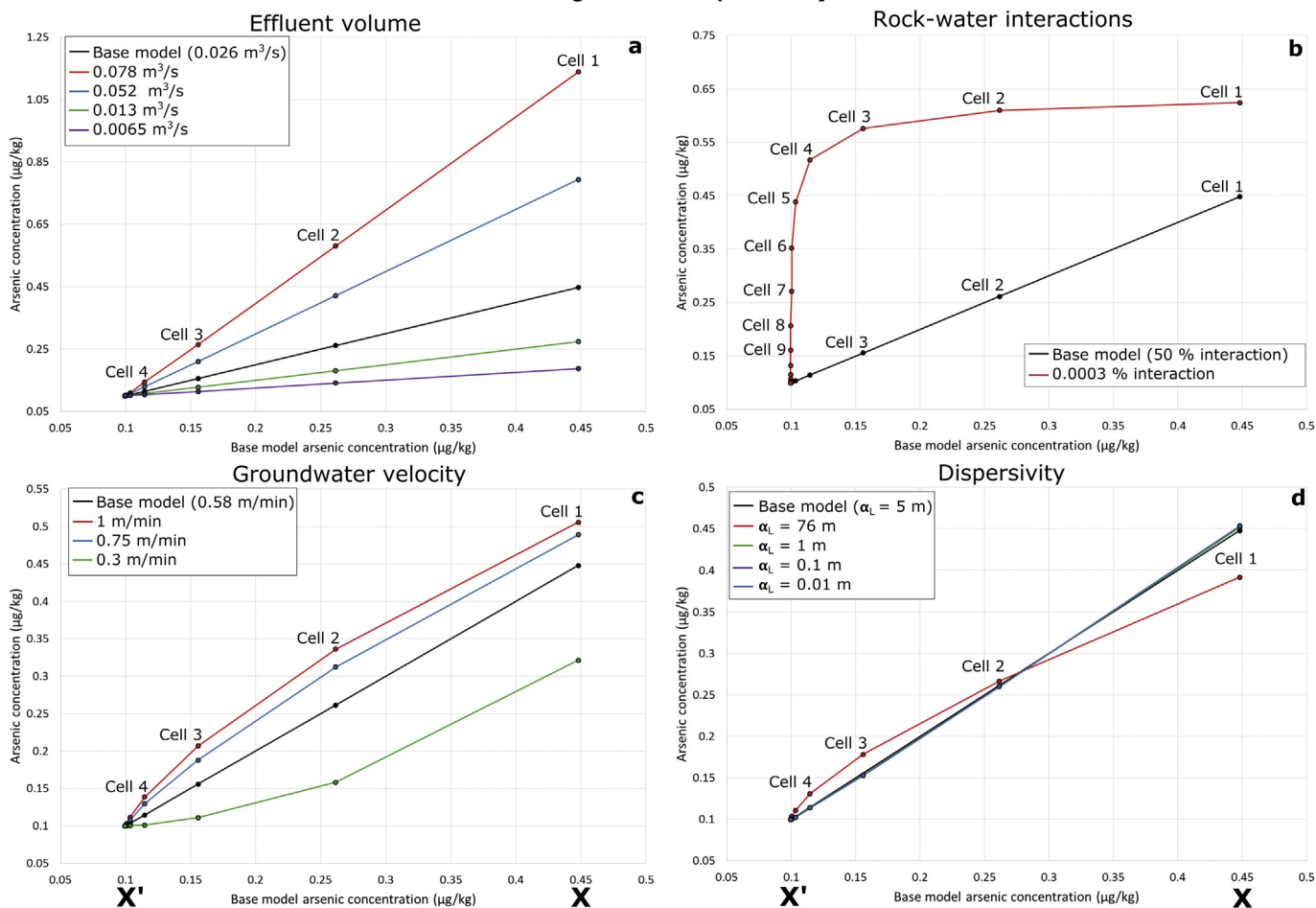


Figure 7. Sensitivity analysis of (a) effluent volume, (b) rock-water interaction, (c) groundwater velocity, and (d) dispersivity. For effluent volume, groundwater velocity, and dispersivity, arsenic concentrations become consistently similar to the base model by cell 5 (500 m from lagoon) at $\sim 0.1 \mu\text{g/kg}$ of solvent.

between arsenic concentration and temperature. Both geothermal and groundwater had the same dominant species of arsenite (H_3AsO_3). After infiltration, arsenite still maintained its dominant chemical forms.

5.2. Dilution processes

According to PHREEQC simulations, when arsenic-rich geothermal waters infiltrated into the subsurface, dilution

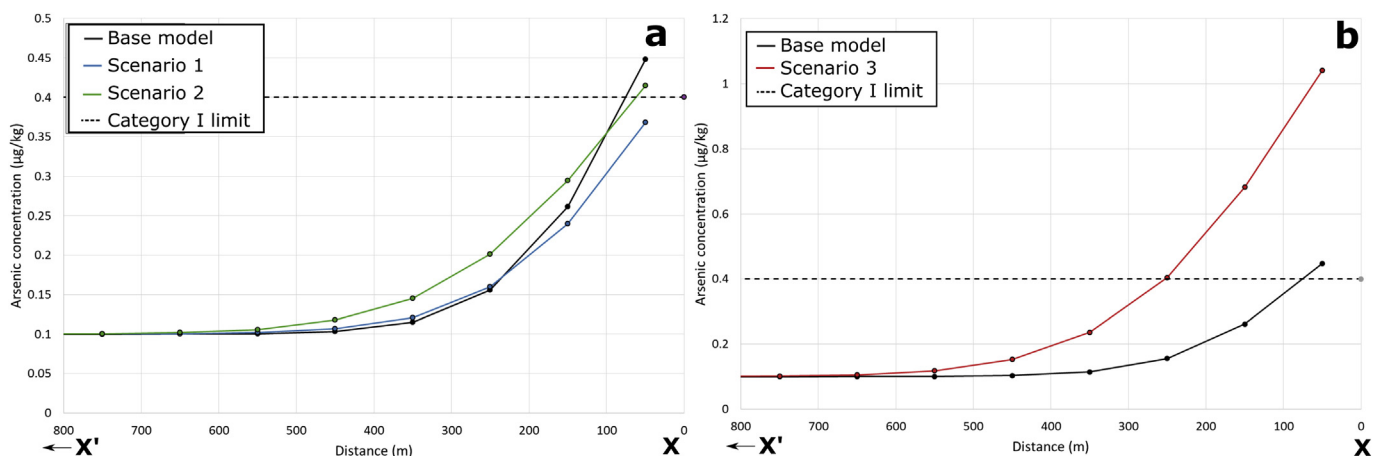


Figure 8. Base model and scenarios along the transect. (a) Comparison of scenarios 1 and 2 with the base model at 20 years; (b) Comparison of scenario 3 with the base model at 20 years.

reduced the arsenic content from ~ 224 to ~ 0.6 $\mu\text{g/kg}$ of solvent. Dilution clearly was an important factor, as it reduced the contaminant concentration level from Category (V) to Category (II) (Umhverfissráðuneytið, 1999).

Increasing power production is most likely to alter the volume of effluent-water released from Bjarnarflag Power Plant. Varying geothermal enthalpies produce different volume of effluent (Hauksson, 2013). Although a three-fold increase in effluent water ($0.078 \text{ m}^3/\text{s}$) from current levels is unrealistic, simulations suggested that dilution would still reduce contamination from ~ 224 to ~ 1.14 $\mu\text{g/kg}$ of solvent (Fig. 7c).

Within the dilution simulation, the saturation state of several important minerals remained unchanged, considering the large-scale dilution (Table 1). SiO_2 remained unsaturated but gibbsite, similar to hydrous iron oxides, became more saturated with the input of geothermal water. In the actual aquifer, pyrite is expected deep within the basaltic aquifer system (Gudmundsson et al., 2010), which may aid in arsenic adsorption.

5.3. Adsorption processes

FeO , SiO_2 and Al_2O_3 rich basaltic glass can cause decreased arsenic mobility at pH 3–10 (Sigfusson et al., 2008). The geochemical similarities of AsO_3^{3-} to H_4SiO_4 should also be considered (e.g. Pascua et al., 2005; Charnock et al., 2007). High phosphate concentrations hinder As^{5+} adsorption, but not As^{3+} adsorption (Dzombak and Morel, 1990). Furthermore, silica competes with arsenic for adsorption sites (Sracek et al., 2004).

For a significant rise in arsenite concentration to occur, an unrealistically low porosity had to be assumed (0.0003%). This may indicate that the basaltic glass either did not operate at its maximum adsorption capacity, or had a strong adsorption capability. We show that adsorption by basaltic glass is very effective even at a very low interaction-rate (Fig. 7b). This corroborates observations from iron oxide adsorption (Smedley and Kinniburgh, 2002; Sracek et al., 2004; Johannesson et al., 2013).

5.4. Transport processes

In the PHREEQC one-dimensional transport modelling, dispersivity and groundwater velocity were subject to a sensitivity study, which builds upon previous work in southern Iceland (Sigfusson et al., 2011).

5.4.1. Dispersivity

Layered scoria dispersivity attenuated the concentration of arsenic along the transect (Fig. 7d). As a result of attenuation, the upstream (towards X) concentration was reduced and the downstream (towards X') was increased. Fracture-flow dispersivities did not induce a significant change in arsenic concentrations along the transect. The dispersivity considered was longitudinal (α_L), with transverse dispersivity not being taken into account. It is reasonable to expect arsenic concentration to generally reduce with the input of transverse dispersivity.

5.4.2. Groundwater velocity

The variation in groundwater velocity resulted in different concentrations predicted along the transect (Fig. 7c). Within the first 500 m of the transect, simulated slower velocities (0.3 m/min) reduced the arsenic concentration more than faster flows (0.75 and 1 m/min) increased the arsenic concentration. Considering dilution was assumed instantaneous and dispersion was assumed constant, the length of time that basaltic glass and arsenic-rich waters

interacted, was a significant factor in the uptake of arsenic into the bulk aquifer material. Groundwater velocities appeared to be the most significant control on the transport model among the factors considered here.

The inter-dependent system of groundwater velocity, dispersivity and adsorption is most likely the key to understanding arsenic behaviour in basaltic aquifers. A system that has high dispersion, an increased exposure to adsorption and a lower groundwater velocity, may result in a lower arsenic concentration. Conversely, a system that has low dispersion, a decreased exposure to adsorption and a faster groundwater velocity, may result in a higher arsenic concentration.

5.5. Is increased geothermal power production a threat to Lake Mývatn?

The geochemical conditions of the lagoon favoured reduced arsenite. Arsenite was significantly decreased from Category (V) to Category (II) contaminant assuming $11 \text{ m}^3/\text{s}$ reached Lake Mývatn (Vatnaskil, 2008), and $0.026 \text{ m}^3/\text{s}$ of effluent was released from the Námafjall geothermal field (Hauksson, 2013). Moreover, when simulating a very high volume of re-injected effluent ($0.078 \text{ m}^3/\text{s}$), the contaminant was still limited to a Category (II) contaminant after dilution.

All three scenarios and the base model were simulated for 20 years (Fig. 7). In all four cases the arsenite concentration reached background levels before the mid-way point of the transect. It appears that basaltic glass is in sufficient supply over a 20-year period. Faster flows replicated fracture-flow pathways, yet differences to the base model were on the scale of ~ 0.2 $\mu\text{g/kg}$ of solvent. A 40-year simulation period also suggested concentrations reached background levels at a safe distance from Lake Mývatn. Considering the faster flow parameter used in this scenario, there appears to be no heightened risk to the lake ecosystem.

The modelling work done in this study may fall short in real representation of field conditions of the basaltic aquifer system. This was only a selection of possible scenarios and further work should be done to assess the combined effect of variables including the arsenic immobilisation effect of SiO_2 and PO_4 with basaltic glass. However, in our extreme-case scenario, there appears to be sufficient adsorption and dilution of arsenic in the aquifer. Landsvirkjun plans to re-inject geothermal effluent at 400 m depth if the power plant is expanded (S. H. Markússon, 2014, personal communication, 1 August). At this depth, the temperature is 100°C according to alteration minerals (Gudmundsson et al., 2010). The model could be improved through simulating an increase in temperature (100°C), by correcting the arsenite diffusion coefficient and equilibrium constants of the arsenic surface reactions. This study also recommends the analysis of adsorption coefficients for competing ions such as SiO_2 . Additional sample sites, sampling, pumping tests, adsorption capability tests, and tracer tests will add further insight into the hydrogeological properties of the Mývatn basalt and provide robust data to constrain the geochemical model.

6. Conclusion

Geothermal demands in Bjarnarflag, northern Iceland, require assessment of the fate of arsenic within the subsurface. The main factor controlling the fate of arsenic is the ability of basaltic glass to adsorb the contaminant in the groundwater system. In dilution simulations arsenite (H_3AsO_3) is decreased to a Category (II) contaminant. In transport simulations, geothermal arsenite did not reach Lake Mývatn, even in the worst-case scenario. This is a consequence of the strong capability of basaltic glass in removing

arsenic from the aqueous phase. This study indicates that the adsorption strength is very high which means that the physical hydrogeological parameters, namely: groundwater velocity and longitudinal dispersivity have less influence on the concentration profile. Considering the limitations, the results give insight into the processes involved within the aquifer system. The results also give reasonable support for re-injection as a suitable solution for geothermal arsenic disposal, in similar basaltic aquifer systems worldwide.

Acknowledgements

We would like to thank Þráinn Friðriksson and Ester Eyjólfsson of the Iceland Geosurvey for providing data. We are grateful for geothermal- and geochemical-related discussion and feedback from Egill Júlíusson, Ásgerður Sigurðardóttir, Bergur Sigfusson, Dominik Weiss and Guðjón Eggertsson. We would like to thank one anonymous reviewer who greatly improved the readability of the manuscript. Finally we'd like to thank Landsvirkjun and the Landsvirkjun Energy Research Fund for supporting this project.

References

- Ármannsson, H., 2005. Monitoring the effect of geothermal effluent from the Krafla and Bjarnarflag power plants on groundwater in the lake Mývatn area, Iceland, with particular reference to natural tracers. In: *Proceedings World Geothermal Congress, (Turkey)*, pp. 1–8.
- Ármannsson, H., Kristmannsdóttir, H., Ólafsson, M., 1998. Krafla – Námafjall. The Effect of Volcanic Activity on Groundwater (In Icelandic). Orkustofnun. OS-98066, p. 33.
- Arnsón, B., 1977. Hydrothermal systems in Iceland traced by deuterium. *Geothermics* 5 (1–4), 125–151.
- Arnórsson, S., 1995. Geothermal systems in Iceland: structure and conceptual models - ii. low-temperature areas. *Geothermics* 24 (5/6), 603–629.
- Arnórsson, S., 2003. Arsenic in surface – and up to 90°C ground waters in a Basalt Area, N-Iceland: processes controlling its mobility. *Applied Geochemistry* 18, 1297–1312.
- Charnock, J.M., Polya, D.A., Gault, A.G., Wogelius, R.A., 2007. Direct EXAFS evidence for incorporation of As₅₊ in the tetrahedral site of natural andraditic garnet. *American Mineralogist* 92 (11–12), 1856–1861.
- De Zeeuw, E., Gislason, G., 1988. The Effect of Volcanic Activity on the Ground Water System in the Námafjall Geothermal Area, NE Iceland. Orkustofnun. OS-88042/J, p. 39.
- Dzombak, D.A., Morel, F.M.M., 1990. Surface Complexation Modeling: Hydrous Ferric Oxide. Wiley, New York.
- Einarsson, M.A., 1972. Evaporation and Potential Evapotranspiration in Iceland. The Icelandic Meteorological Office Reykjavík.
- Einarsson, Á., Stefánsdóttir, G., Jóhannesson, H., Ólafsson, J.S., Gislason, G.M., Wakana, I., Gudbergsson, G., Gardarsson, A., 2004. The ecology of Lake Mývatn and the River Laxá: variation in space and time. *Aquatic Ecology* 38, 317–348.
- Fendorf, S., Michael, H.A., van Geen, A., 2010. Spatial and temporal variations of groundwater arsenic in south and Southeast Asia. *Science* 328, 1123–1127.
- Ferguson, J.F., Gavis, J., 1972. A review of the arsenic cycle in natural waters. *Water Research* 6, 1259–1274.
- Franzson, H., Guðfinnsson, G.H., Helgadóttir, H.M., Frolova, J., 2010. Porosity, Density and Chemical Composition Relationships in Altered Icelandic Hyaloclastites. *Water-Rock Interaction*, pp. 199–202.
- Fridleifsson, I.B., 2001. Geothermal energy for the benefit of the people. *Renewable and Sustainable Energy Reviews* 5 (3), 299–312.
- Guðmundsson, A., Mortensen, A.K., Hjartarson, A., Karlsdóttir, R., Ármannsson, H., 2010. Exploration and utilization of the Námafjall high temperature area in N-Iceland. In: *Proceedings World Geothermal Congress, (Bali, Indonesia)*, pp. 25–29.
- Guðmundsson, G., Pálmason, G., Grönvold, K., Ragnars, K., Sæmundsson, K., Arnórsson, S., 1971. Námafjall – Krafla: Áfangaskýrsla Um Rannsókn Jarðhitasvæðanna. Orkustofnun, p. 121.
- Hauksdóttir, S., Kristmannsdóttir, H., Axelsson, G., Ármannsson, H., Bjarnason, H., Ólafsson, M., 2000. The influence of effluent water discharged from the Námafjall Geothermal field on local groundwater. In: *Proceedings World Geothermal Congress, (Japan)*, pp. 603–608.
- Hauksón, T., 2013. Krafla Og Bjarnarflag – Afköst Borhola Og Efnainnihald Vatns Og Gufu Í Borholum Og Vinnslurás Árið 2012. Landsvirkjun, LV-2013-07, p. 75.
- Johannesson, K.H., Dave, H.B., Mohajerin, T.J., Datta, S., 2013. Controls on tungsten concentrations in groundwater flow systems: the role of adsorption, aquifer sediment Fe(III) oxide/oxyhydroxide content, and thiotungstate formation. *Chemical Geology* 351, 76–94.
- Kristmannsdóttir, H., Ármannsson, H., Hauksdóttir, S., Axelsson, G., Ólafsson, M., Guðmundsdóttir, H., 2001. Grunnvatnsrannsóknir Á Mývatnssvæðinu. Orkuþing, pp. 53–559.
- Nickson, R., McArthur, J.M., Burgess, W.G., Ahmed, K.M., Ravenscroft, P., Rahman, M., 1998. Arsenic poisoning in Bangladesh groundwater. *Nature* 395, 338.
- Nimmer, R.E., 1998. Ground Water Tracer Studies in Columbia River Basalt. M.S. Thesis. Department of Geological Sciences, University of Idaho.
- Ólafsson, J., 1979a. Physical characteristics of Lake Mývatn and river Laxá. *Oikos* 32, 38–66.
- Ólafsson, J., 1979b. The chemistry of Lake Mývatn and river Laxá. *Oikos* 32, 82–112.
- Parkhurst, D.L., Appelo, C.A.J., 1999. User's Guide to PHREEQC (Version 2) – A Computer Program for Speciation, Batch-Reaction, One-Dimensional Transport, and Inverse Geochemical Calculations. U.S. Geological Survey, p. 326.
- Pascua, C., Charnock, J., Polya, D.A., Sato, T., Yokoyama, S., Minato, M., 2005. Arsenic-bearing smectite from the geothermal environment. *Mineralogical Magazine* 69 (5), 897–906.
- Pierce, M.L., Moore, C.M., 1982. Adsorption of arsenite and arsenate on amorphous iron hydroxide. *Water Research* 16, 1247–1253.
- Ravenscroft, P., Brammer, H., Richards, K.S., 2009. Arsenic Pollution: a Global Synthesis, first ed. Wiley-Blackwell, UK.
- Robinson, B., Outred, H., Brooks, R., Kirkman, J., 1995. The distribution and fate of arsenic in the Waikato River system, North Island, New Zealand. *Chemical Speciation and Bioavailability* 7 (3), 89–96.
- Schulze-Makuch, D., 2005. Longitudinal dispersivity data and implications for scaling behavior. *Ground Water* 43 (3), 443–456.
- Sigfusson, B., Meharg, A.A., Gislason, S.R., 2008. Regulation of arsenic mobility on basaltic glass surfaces by speciation and pH. *Environmental Science & Technology* 42 (23), 8816–8821.
- Sigfusson, B., Gislason, S.R., Meharg, A.A., 2011. A field and reactive transport model study of arsenic in a basaltic rock aquifer. *Applied Geochemistry* 26 (4), 553–564.
- Smedley, P., Kinniburgh, D., 2002. A review of the source, behaviour and distribution of arsenic in natural waters. *Applied Geochemistry* 17 (5), 517–568.
- Souza, W.R., Voss, C.I., 1987. Analysis of an anisotropic coastal aquifer system using variable-density flow and solute transport simulations. *Journal of Hydrology* 92 (1–2), 17–41.
- Squibb, K.S., Fowler, B.A., 1983. The toxicity of arsenic and its compounds. In: Fowler, B.A. (Ed.), *Biological and Environmental Effects of Arsenic*. Elsevier, New York.
- Sracek, O., Bhattacharya, P., Jacks, G., Gustafsson, J.-P., Brömssen, M.V., 2004. Behavior of arsenic and geochemical modelling of arsenic enrichment in aqueous environments. *Applied Geochemistry* 19 (2), 169–180.
- Steele, T.D., Kunkel, J.R., Way, S.C., Koenig, R.A., 1989. Flow of Groundwater and Transport of Contaminants through Saturated Fractured Geologic Media. NUREG/CR-5391. U.S. Nuclear Regulatory Commission, Washington, DC.
- Sæmundsson, K., 2010. Námafjall. Geological and Geothermal Map, 1:25,000. Landsvirkjun and Iceland GeoSurvey.
- Thorarinnsson, S., 1979. The postglacial history of the Mývatn area. *Oikos* 32, 17–28.
- Þóroddsson, F., Sigbjarnarson, G., 1983. The Diatomite Plant by Lake Mývatn. *Groundwater Studies (In Icelandic)*. Orkustofnun. OS-83118/V, p. 41.
- Umhverfisráðuneytið, 1999. Reglugerð um varnir gegn mengun vatns nr. 796/1999 með síðari breytingum nr. 533/2001 og nr. 913/2003. Stjórnartíðindi, B 106, Nr. 785-810, s. 2231–2253. <https://www.reglugerid.is/reglugerdir/eftir-raduneytum/umhverfisraduneyti/nr/4482>.
- Vatnaskil, V., 2008. Norðausturland. Lokaskýrsla um gerð grunnvatnslíkans í gosbeltinu norðan við Kröflu. Verkfræðistofan Vatnaskil.
- Webster, J.G., Nordstrom, D.K., 2003. Geothermal Arsenic – the source, transport and fate of arsenic in geothermal systems. In: Welch, A., Stollenwerk, G. (Eds.), Chapter 4 in "Arsenic in Ground Water", pp. 101–125.
- Welch, A.H., Westjohn, D.B., Helsel, D.R., Wanty, R.B., 2000. Arsenic in ground water of the United States: occurrence and geochemistry. *Ground Water* 38 (4), 589–604.
- Willis, S.S., Haque, S.E., Johannesson, K.H., 2011. Arsenic and antimony in groundwater flow systems: a comparative study. *Aquatic Geochemistry* 17, 775–807.
- World Health Organisation, 2011. Arsenic in Drinking-Water: Background Document for Development of WHO Guidelines for Drinking-Water Quality (WHO/SDE/WSH/03.04/75/Rev/1).